CONVERGENCE OF THE EKF IN MARK-BASED VISION FOR 3D VEHICLE TRACKING

E. Delgado, A. Barreiro[†], J.A. Baltar[††]

E.T.S. Ingenieros Industriales. University of Vigo. 36200-Vigo (Spain)
e-mail: emma@aisa.uvigo.es, [†]abarreiro@uvigo.es, [††]jbaltar@aisa.uvigo.es

Abstract: In this paper, the extended Kalman filtering (EKF) technique is considered for 3-dimensional tracking of vehicle movement using a fixed camera that provides vehicle images showing several marks, easily detectable, fixed to the vehicle body. The algorithm will be implemented in a minihelicopter hover-stabilization application. For this problem, we present results on the convergence and the domain of attraction of the non-linear observation scheme as a function of the tuning filter parameters: the initial value of the covariance and the robustifying parameter α. *Copyright © 2005 IFAC*

Keywords: Dynamic vision, Nonlinear observers, Extended Kalman Filters, Domain of attraction, Convergence, Vehicle tracking, Pose estimation.

1. INTRODUCTION

This work belongs to a project devoted to the control and stabilization of a minihelicopter in *hover* (fixed position) in an experimental platform. The position and orientation of the vehicle are measured by vision, recording frames in which there are several marks, made easily detectable in some way, *e.g.*, bright-light marks in a dim-light ambient. In this way, the vision system operates as a position sensor for 3D tracking (for more details see Appendix A). This concept is also known in the literature as *dynamic vision* or *vision-in-the-loop* (Azarbayejani and Pentland, 1995; Soatto, *et.al.*, 1996), with applications in numerous fields: robotics, control, …

Our approach is based on optimal state estimation and Extended Kalman Filter (EKF) (Dorato *et.al.*, 1995), which can be interpreted as a nonlinear state observer (Delgado and Barreiro, 2003).

In many navigation applications, the state dynamics (right-hand-side of $dx/dt=f(x, ...)$) are known, using inertial sensors, and in this way, the EKF provides sensor fusion between absolute and relative measurements. However, in dynamic vision, no inertial information is avaliable.

The only approach, widely used (Azerbayejani and Petland, 1995; Soatto *et.al.*, 1996) is to postulate a randomly excited movement in the form $dx/dt=\delta(t)$, with $\delta(t)$ being some kind of random or unknown excitation. In practice, even if $\delta(t)$ is deterministic, the fast convergence of EKF guarantees correct tracking.

In this context, the objective of this paper is to determine the influence and the optimal values of the main parameters on the robustness of the nonlinear observation scheme. So, the size of the domain of attraction (DOA) of the EKF is calculated for a wide range values of the tuning parameters: the initial value of the covariance and the robustifying parameter α. This will allow us to select their optimal values in order to guarantee the convergence of the
EKF and so to estimate the *pose* or 6-dimensional state x (position and euler angles of vehicle).

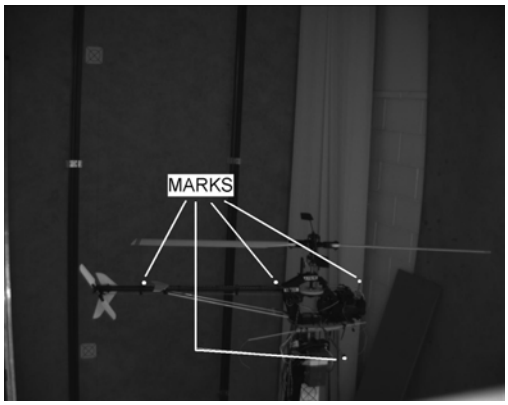

Fig. 1. Vision as a sensor providing the pixel coordinates of the fixed, visible marks.

This paper is an extension of our previous work (Baltar, *et al*., 2004). In this case, the analysis is made over real images of the helicopter with four bright-light marks (see Fig.1), incorporating the lens distortion in the filter measurement equations. Besides of, we estimate the domain of attraction as a function of the tuning parameters.

The content of the paper is as follow. In section 2, an overall description of the system is introduced. The nonlinear observer EKF applied to mark-based vision for vehicle tracking is developed in section 3. After that, is obtained through simulations the domain of attraction in the observer in section 4, and finally conclusions are discussed in section 5.

2. MARK-BASED VISION FOR 3D VEHICLE TRACKING

The principal objective of this task is to obtain the state of movement of a rigid solid using an image sequence captured from a fixed camera. In order to reducing pre-process, the rigid solid has marks that can be easily localizable in the image.

Once we capture an image of the scene and after the extraction algorithm, the pixel coordinates on the image plane of each of *m* marks attached to the helicopter, are obtained. Based on these measures and postulating the state dynamic as a randomly excited movement, we can estimate the current state (*pose* of the vehicle*)* by running the Kalman filter. So, the state equation is in the form:

$$\dot{x}(t) = \delta(t) \tag{1}$$

The signal δ can be considered $\delta \approx N(0,Q)$, that is, zero-mean gaussian noise with covariance $Q > 0$, and the state (pose) x is a six-dimensional vector formed by the three translation $T(t)=(t_x(t),t_y(t),t_z(t))$ and the three Euler angles $E(t)=(\phi(t),\theta(t),\psi(t))$:

$$x(t) = \begin{pmatrix} t_x(t) & t_y(t) & t_z(t) & \phi(t) & \theta(t) & \psi(t) \end{pmatrix}^T \tag{2}$$

The relation between the Euler angles $\phi(t)$, $\theta(t)$, $\psi(t)$ (roll, pitch, yaw) and the rotation matrix $R(t)$ in SO(3) is (Sastry, 1999):

$$R(t) = \exp(R_z\psi(t)) \cdot \exp(R_y\theta(t)) \cdot \exp(R_x\phi(t)) \tag{3}$$

Where R_x, R_y, R_z are the partial derivatives of the rotation matrix $R_x = \hat{e}_1$, $R_y = \hat{e}_2$, $R_z = \hat{e}_3$, with the canonical base e_1, e_2, e_3, and:

$$\hat{\begin{pmatrix} \omega_1 \\ \omega_2 \\ \omega_3 \end{pmatrix}} = \begin{pmatrix} 0 & -\omega_3 & \omega_2 \\ \omega_3 & 0 & -\omega_1 \\ -\omega_2 & \omega_1 & 0 \end{pmatrix} \tag{4}$$

Now, the measurement equations are Eq.(5) below, where $h_j(x(t))$, with $1 \le j \le m$ is the normalized (pinhole) image projection of each of the *m* marks in pixel coordinates, after including lens distortion. The signal $\varepsilon_{(t)} = (\varepsilon_1(t) , \ldots, \varepsilon_m(t))^T$ is the measurement noise, usually assumed to be $\varepsilon \approx N(0,\Theta)$, with $\Theta > 0$.

$$y(t) = \begin{pmatrix} y_1(t) \\ \vdots \\ y_m(t) \end{pmatrix} = h(x(t)) + \varepsilon(t) = \begin{pmatrix} h_1(x(t)) \\ \vdots \\ h_m(x(t)) \end{pmatrix} + \varepsilon(t) \tag{5}$$

Assume the case of *m* marks that are always visible and their distribution in the object is known (consider the Fig.1), this is, their coordinates in local (helicopter) reference are:

$$X_O^{(j)} = \begin{pmatrix} x_O^{(j)} \\ y_O^{(j)} \\ z_O^{(j)} \end{pmatrix}, j = 1,\ldots m \tag{6}$$

Then, the marks coordinates in global (world) reference are:

$$X_C^{(j)}(t) = \begin{pmatrix} x_C^{(j)}(t) \\ y_C^{(j)}(t) \\ z_C^{(j)}(t) \end{pmatrix} = h_C^{(j)}(T(t),R(t)) = T(t) + R(t)X_O^{(j)} \tag{7}$$

where $T(t)$ and $R(t)$ are the time dependent traslation and rotation between the mobile object and the fixed camera.

Let us project now the marks on the image plane according to the intrinsic parameters of our camera (with a second order symmetric radial distortion model obtained with the *Camera Calibration Toolbox for Matlab*, free software avaliable in: http:/www.vision.caltech.edu/bouguetj/).

First, the normalized (pinhole) image projection are:

$$n^{(j)}(t) = \begin{pmatrix} x_n^{(j)}(t) \\ y_n^{(j)}(t) \end{pmatrix} = h_n^{(j)}(X_C^{(j)}(t)) = \begin{pmatrix} x_c^{(j)}(t)/z_c^{(j)}(t) \\ y_c^{(j)}(t)/z_c^{(j)}(t) \end{pmatrix} \tag{8}$$

After including lens distortion, and letting $r^2 = x_n^2 + y_n^2$, the new distortioned marks coordinates:

$$d^{(j)}(t) = \begin{pmatrix} x_d^{(j)}(t) \\ y_d^{(j)}(t) \end{pmatrix} = h_d^{(j)}(n^{(j)}(t)) = \left(1 + Kc_1 \cdot r^2\right) \cdot n^{(j)}(t) \quad (9)$$

With Kc_1 = -0.19457 the coefficient of second order radial distortion term. Once distortion is applied, the final pixel coordinates of the projections of the *m* marks are:

$$y^{(j)}(t) = \begin{pmatrix} u^{(j)}(t) \\ v^{(j)}(t) \end{pmatrix} = h_p^{(j)}(d^{(j)}(t)) = \begin{pmatrix} l_x \cdot x_d^{(j)}(t) + o_x \\ l_y \cdot y_d^{(j)}(t) + o_y \end{pmatrix} \quad (10)$$

Where $l = (l_x \;\; l_y)^T = (1865.33 \;\; 1868.57)^T$ is the focal length and o_x = 510.68 and o_y = 619.68 the principal point in pixel coordinates obtained by the calibration procedure.

Now, the problem to solve in dynamic vision can be formulated more accurately: "From the vision registers $y_j(t)$, determine estimations $\hat{x}(t)$ of the object movement $x(t)$ along time".

3. OBSERVER EKF IN DYNAMIC VISION

The 3D *pose* estimation problem using nonlinear observer EKF, can be formalized as follows. Assume that the plant dynamics, with $f(x(t),t) = 0$, can be written as:

$$\begin{cases} \dot{x}(t) = \delta(t) \\ y(t) = h(x(t)) + \varepsilon(t) \end{cases} \quad (11)$$

where $\delta(t)$ and $\varepsilon(t)$ represent the typical state and measurement noise. The solution of Eq. (11) from a nominal initial state $x(0) = \bar{x}_0$ defines the nominal state trajectory. The EKF observer gives estimations $\hat{x}(t)$ of the state $x(t)$ by running the dynamics:

$$\begin{cases} \dot{\hat{x}} = K(t)(y(t) - \hat{y}(t)) \\ \hat{x}(0) = \hat{x}_0 \\ \hat{y}(t) = h(\hat{x}(t)) \end{cases} \quad (12)$$

started at $\hat{x}(0) = \hat{x}_0$. The estimation error is $\zeta(t) = \hat{x}(t) - \bar{x}(t)$, started at $\zeta_0 = \hat{x}_0 - \bar{x}_0$. In the extended Kalman filter, the Jacobians of *f, h,* are evaluated at the estimated trajectory $\hat{x}(t) = \bar{x}(t) + \zeta(t)$. So, let us introduce:

$$\begin{aligned} A(\zeta,t) &= \frac{\partial f}{\partial x}\left(\bar{x}(t) + \zeta, t\right) = 0 \\ C(\zeta,t) &= \frac{\partial h}{\partial x}\left(\bar{x}(t) + \zeta\right) \\ B(\zeta,t) &= C^T(\zeta,t)\Theta^{-1}C(\zeta,t) \end{aligned} \quad (13)$$

Remark 1. Notice that we do not impose directly on $f(\cdot)$, $h(\cdot)$ detectability conditions. If the system is not detectable, this problem appears indirectly because the covariance matrix *P* becomes unbounded.

The varying Kalman gain used in Eq. (12) is:

$$K(t) = P(t)C^T(\zeta(t),t)\Theta^{-1} \quad (14)$$

where the symmetric, positive definite covariance matrix *P(t)* is the solution of the differential Riccati equation:

$$\begin{cases} \dot{P} = 2\alpha P(t) - P(t)B(\zeta(t),t)P(t) + Q \\ P(0) = P_0 \end{cases} \quad (15)$$

started at some $P_o > 0$. The term $2\alpha P(t)$ comes from:

$$2\alpha P(t) = A_\alpha(\zeta(t),t)P(t) + P(t)A_\alpha^T(\zeta(t),t) \quad (16)$$

With:

$$A_\alpha(\zeta,t) = A(\zeta,t) + \alpha I = \alpha I, \qquad A(\zeta,t) = 0 \quad (17)$$

where $\alpha > 0$, is an exponential weighting factor introduced following (Safonov, 1980) to make more robust the EKF. In our framework, $Q, \Theta > 0$ can be regarded as matrices representing the covariance of the state and measurement noise.

Remark 2. The matrix *C,* the Jacobian of the measurement function *h*, is obtained by applying the chain rule (we do not write the *j* and *t* dependence) to $y=h(x)=h_p(h_d(h_n(h_c(T,R(\phi,\theta,\psi)))))$:

$$C_j = \frac{\partial h_j}{\partial x} = \begin{pmatrix} l_x & 0 \\ 0 & l_y \end{pmatrix} \cdot \begin{pmatrix} 1 + 3Kc_1x_n^2 + Kc_1y_n^2 & 2Kc_1x_ny_n \\ 2Kc_1x_ny_n & 1 + Kc_1x_n^2 + 3Kc_1y_n^2 \end{pmatrix} \cdot \begin{pmatrix} \frac{1}{z_c} & 0 & -\frac{x_c}{z_c^2} \\ 0 & \frac{1}{z_c} & -\frac{y_c}{z_c^2} \end{pmatrix} \cdot \left(I_{3\times3} \;\; \frac{\partial R}{\partial \phi}X_o \;\; \frac{\partial R}{\partial \theta}X_o \;\; \frac{\partial R}{\partial \psi}X_o\right) \quad (18)$$

Where, from Eq. (3):

$$\begin{aligned} &\frac{\partial R}{\partial \phi} = R \cdot R_x, \quad \frac{\partial R}{\partial \psi} = R_z \cdot R \\ &\frac{\partial R}{\partial \theta} = R \cdot \exp\left(R_x^T \cdot \theta(t)\right) \cdot R_y \cdot \exp\left(R_x \cdot \phi(t)\right) \end{aligned} \quad (19)$$

So, *Cj* results in a 2 by 6 matrix. Joining the row pairs that agree with the displayed coordinates for the *m* marks, the complete matrix of 2m by 6 size is obtained: $C = \frac{\partial h}{\partial x}(\hat{x})$.

4. EKF: DOMAIN OF ATTRACTION

A useful way of measuring the robustness of the EKF for some choice of the filter parameters is to

determine an estimation of the Domain of Attraction (DOA).

The notion of Domain of Attraction is conceptually simple. First, assume that the plant in Eq. (11) is operating at a constant nominal point $x = \bar{x}$, $y = \bar{y} = h(\bar{x})$, without noise ($\delta = \varepsilon = 0$). Second, it can be seen that the EKF in Eq. (12) has as equilibrium point also $\hat{x} = \bar{x}$, $\hat{y} = \bar{y}$, the question is how robust is this equilibrium.

To check robustness, consider that we do not know that $x = \bar{x}$, so we guess some $\hat{x}_0 \neq \bar{x}$, then we run the EKF dynamics Eqs. (12-15). If $\hat{x}_0 \approx \bar{x}$, then very likely $\hat{x}(t) \to \bar{x}$. But if $\hat{x}_0 - \bar{x}$ is large, it may happen that $\hat{x}(t)$ diverge to another value or to infinity. The DOA is the set of all those $\hat{x}_0$ such that $\hat{x}(t) \to \bar{x}$. Obviously, it is important to have large DOAs because it is better if we have large initial errors $\hat{x}_0 - \bar{x}$ or large transients of the δ ,ε in (11) producing large deviations of the actual *x* around $\bar{x}$.

But the DOA is, in general, very difficult to compute exactly. We prefer to address estimations of the DOA. Simple estimations of the DOA are obtained from hypercubes in the state-space. In our 6-dimensional case, let us consider all the 64 vertex obtained from sign-combinations in:

$$\zeta_0 = \hat{x}_0 - \bar{x} = m_\zeta \cdot (\pm 1, \pm 1, \pm 1, \pm 1, \pm 1, \pm 1) \qquad (20)$$

For each m_ζ we define a boolean function $\varphi(m_\zeta)$ for convergence, where:

$$\varphi(m_\zeta) = \begin{cases} 1 & \text{if all the 64 trajectories converge} \\ 0 & \text{if any of the trajectories diverges} \end{cases} \qquad (21)$$

Then, $M_\zeta(P_0, \alpha)$ in the following equation is a measure of the size of the DOA for the values P_0, α, considered in the observer Eqs. (12-15):

$$M_\zeta(P_0, \alpha) = \max\{m_\zeta : \varphi(m_\zeta) = 1\} \qquad (22)$$

So, in order to estimate the DOA of the EKF applied to the mark-based vision for 3D vehicle tracking, we select any captured image of the scene.

After the extraction algorithm, the initial data are the pixel coordinates on the image plane of each of *m* = 4 marks attached to the helicopter. (Note that with three marks not collinear it is possible to obtain the 6-DOF of the state). So this number and distribution of the marks form a basic observable configuration in our problem. Studies relatives to this issue can be seen in (Weng *et.al.*, 1993).

We consider then a constant state $\bar{x}$ and no measurement noise: δ=0 and ε=0 in Eq. (11).

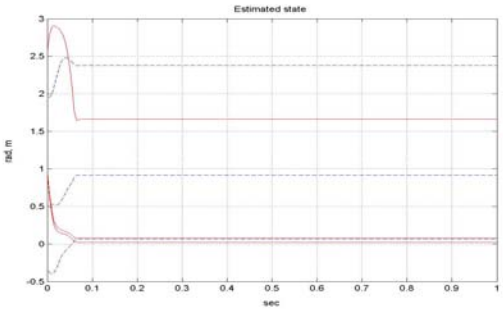

Fig. 2. Current estimated state by running the EKF. Translational components (solid) and Euler angles (dashed).

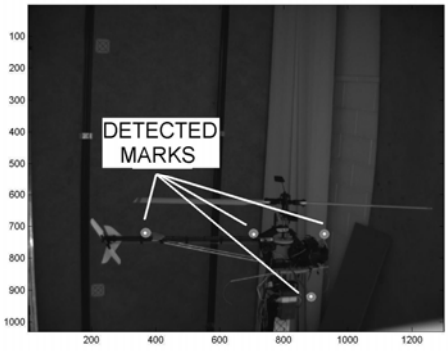

Fig. 3. Testing the obtained pose (current state).

The Q matrix that represents the covariance of the state, is selected as a diagonal matrix considering a translation velocity deviation $\sigma_T^2 = 0.1^2$ (m/sec)^2 and a rotational velocity deviation $\sigma_E^2 = 0.1396^2$ (rad/sec)^2:

$$Q = diag(\sigma_T^2, \sigma_T^2, \sigma_T^2, \sigma_E^2, \sigma_E^2, \sigma_E^2) \qquad (23)$$

In the same way the matrix $R = \sigma_p^2 * I_{2m \times 2m}$, asssociated to the covariance of the measurement, is seleted with $\sigma_p^2 = 2^2$, in *pixel* units.

So, after defining some adequate values of the design parameters (initial covariance P_0 and the weighting factor α) by running the Kalman filter (sample period
dt = 0.005 sec) with a non zero initial estimation error, we can estimate the current state (*pose* of the helicopter).This can be seen in the figures Fig.2 and Fig.3.

An important question is to find the optimal values of the main parameters on the robustness of the nonlinear observation scheme: P_0 and α.

So, the size of the domain of attraction (DOA) of the EKF is calculated for a wide range values of these parameters:

$$P_0 = v_g \cdot Q, \quad v_g = 10^{-4} : 5 \cdot 10^{-3} : 6 \cdot 10^{-2} \qquad (24)$$

$$\alpha = 5 : 5 : 125 \qquad (25)$$

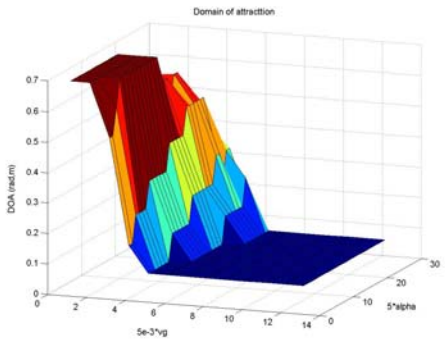

Fig. 4. DOA in EKF as a function of the design parameters P_0 and α

For this purpose, for all the values P_0 and α defined in Eq. (24) and Eq. (25), we increase the initial estimation error, testing that all the trajectories that result after considering the hypercube in Eq. (20) converge (tend to nominal state). The process continues while the convergence is guaranteed. Finally we obtain, for each pair of values P_0 and α, the maximum estimation error with guaranteed convergence $M_\zeta(P_0,\alpha)$.

The results of these extensive simulations are summarized in the figure Fig. 4. Here we can see that for values of $v_g > 0.035$, the size of the DOA is constant with a very small value although the α value
increases. The best results are obtained for $0.01 \leq vg \leq 0.02$. In this range of v_g values if we increase the α parameter, the DOA increases also, and allows for initial estimation errors until $M_\zeta(P_0,\alpha)$=0.6 *rad*, *m* (with any combined signed in all the state variables).

In fact the possibility of increasing α, of course maintaining an acceptable size of DOA with guaranteed convergence, is important to reduce the time of convergence in the observer. This is shown in the figure Fig. 5. This graphic is calculated finding in each case the time in which the estimation error remains smaller than 0.0087 *rad*, *m*. In all cases, the result saved is the worst value obtained in the studied hypercube. For values between $50 \leq \alpha \leq 100$ the time reduction is important and in practice the variation due to change v_g value (inside intervall $0.01 \leq vg \leq 0.02$) is negligible.

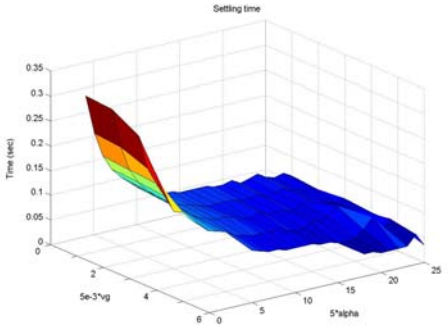

Fig. 5. Settling time in EKF as a function of the design parameters P_0 and α

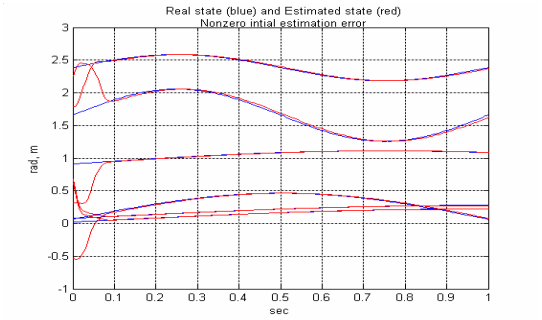

Fig. 6. Real state (thin) and estimated state (thick) by EKF along the time, with nonzero initial estimation error.

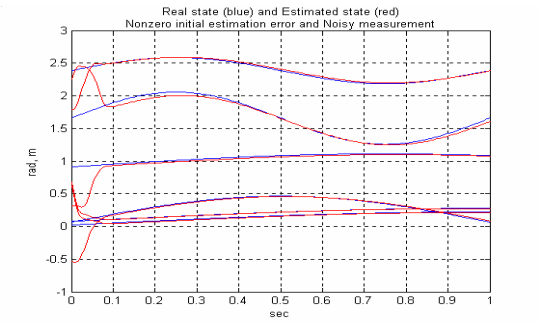

Fig. 7. Real state (thin) and estimated state (thick) by EKF along the time, with nonzero initial estimation error and noisy measurements.

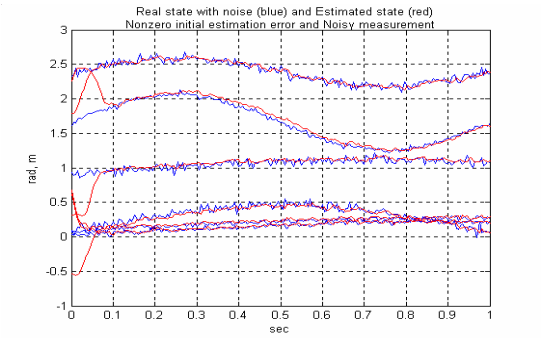

Fig. 8. Real state with noise (thin) and estimated state (thick) by EKF along the time, with nonzero initial estimation error and noisy measurements.

Finally as an example of performance, with the optimal values previously obtained, the figures Fig. 6, Fig. 7 and Fig. 8 show simulations on how the EKF estimates the object movement along the time. In the Fig.6, we consider nonzero initial estimation error. Then, in the Fig.7, we test the filter incorporating also noisy mesurements. The last simulation (Fig. 8) adds noise to state dynamic.

5. CONCLUSIONS

This paper has reported a convergence analysis of the extended Kalman observer applied to mark-based vision for 3D vehicle tracking.

The main contribution of the paper is to establish, through extensive simulations in *Matlab,* the domain of attraction of the EKF as a function of the tuning

parameters in a basic observable configuration (we assume the case of m=4 marks that are always visible and their distribution in the object is known). This allows us to introduce in the design phase of the filter conditions such as maximum initial estimation error in which the convergence is guaranteed and the time in which this occurs. These aspects are essential in order to finally implement the observer scheme in the general project devoted to the control and stabilization of a minihelicopter.

In this way, the current configuration of our experimental platform has seven marks attached to the helicopter and the vision system is composed by two digital cameras that provide redundancy in the measurements fused into Kalman filter to obtain more reliable estimates of the state. Like this, we assure the minimum number of marks and also it is possible to treat the oclussions because knowing the estimated state in each iteration, we can project the expected pixel coordinates in the next frame. All of this, with the same optimal values previously obtained by simulations.

ACKNOWLEDGEMENTS

Work supported by CICYT, Spain under project DPI02-04401.

REFERENCES

Avila J.C., B.Brogliato, A. Dzul and R. Lozano (2003). Nonlinear modelling and control of helicopters. *Automatica*, **39(9)**, pp. 1583-1596 .

Azarbayejani A. and A.P. Pentland (1995). Recursive estimation of motion, structure, and focal length. *IEEE Trans. On Pattern Analysis and Machine Intelligence,* **17**.

Baltar J.A., E. Delgado and A. Barreiro (2004). Mark-based vision for 3D vehicle tracking using least-squares and Kalman filter. *World Automation Congress WAC'04,* Seville, Spain.

Delgado E. and A. Barreiro (2003). Sonar-based robot navigation using nonlinear robust observer. *Automatica*, **39(7)**, pp. 1195-1203 .

Delgado E. and A. Barreiro (2004). Sonar-based robot navigation using nonlinear robust discrete-time observers. *International Journal of Control*, **77(7)**, pp. 693-702.

Dorato P., C.H. Abdallah and V. Cerone (1995). *Linear-Quadratic Control. An introduction*. Prentice-Hall.

Safonov M.G. (1980). *Stability and Robustness of Multivariable Feedback Systems.* MIT Press.

Sastry S. (1999). *Nonlinear Systems. Analysis, Stability and Control.* Springer-Verlag.

Soatto S., R. Frezza, P. Perona (1996). Motion estimation via dynamic vision. *IEEE Trans. On Autom. Control*, **41**, pp. 393-413.

Weng J., T.S. Huang and N. Ahuja (1993). *Motion and structure from image sequences.* Springer-Verlag.

APPENDIX A

The experimental platform used restricts the number of degrees of freedom. The movements that the helicopter can do are vertical displacement and rotation around vertical axe. This physical implementation for a restricted 2DOF system is similar to that in (Avila *et.al.*, 2003).

The helicopter we use is a *Mikado Logo 20* with a brushless electrical motor and four *Futaba* digital servos connected to the receiver. The vision system is composed by two industrial digital cameras from *Basler*, model *A 101f*, which have a 1300x1030 resolution and a 12 fps rate at the maximum resolution. The images are transmitted through an IEEE-1394 bus to PC with a Windows 2000 operative system (the camera driver imposes us this operative system). In this PC, a C/C++ application shows the images and the localized marks and calculates their pixel coordinates on the image plane.

The pixel coordinates captured by the vision system with a rate of 1/30 *sec*. is transmitted through a custom bus towards an *IDT72241* 4096x9 bit FIFO memory that makes the synchronization easier.

An IBM compatible computer that reads the pixel coordinates stored in the FIFO memory forms the control PC system. In this PC are implemented the state estimation (with fixed sample period dt = 0.005 *sec*.) and control algorithms with a real time arrange in a Windows platform, using the Real Time Windows Target from Matlab/Simulink. The output of this control system is the actuation for the sticks in the radio system. The application is programmed in Simulink and some C subroutines as Simulink S-functions.

The same FIFO simple system is used for transmitting the servos setpoints to the RF system.

A microchip *PIC18F452* microcontroller reads servos needed movements and transmits them in a Pulse Position Modulation to the *Futaba FF9* (nine channels) radio frequency transmitter through a bus that connects in the radio by a proprietary connector.

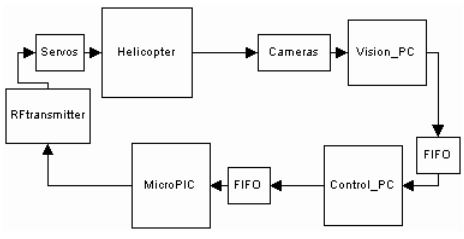

Fig. 9. General layout scheme.